promoting access to White Rose research papers

Universities of Leeds, Sheffield and York
http://eprints.whiterose.ac.uk/

This is an author produced version of a paper published in **Journal of Applied Physics.**

White Rose Research Online URL for this paper:
http://eprints.whiterose.ac.uk/8488/

Published paper
Nabavi, E., Badcock, T.J., Nuytten, T., Liu, H.Y., Hopkinson, M., Moshchalkov, V.V. and Mowbray, D.J. (2009) *Magneto-optical study of thermally annealed InAs-InGaAs-GaAs self-assembled quantum dots.* Journal of Applied Physics, 105 (5). Art. No.053512.
http://dx.doi.org/10.1063/1.3082012

White Rose Research Online
eprints@whiterose.ac.uk

Magneto-optical study of thermally annealed InAs-InGaAs-GaAs self assembled quantum dots

E. Nabavi[1], T J Badcock[2], T. Nuytten[3], H. Y. Liu[4], M. Hopkinson[5], V. V. Moshchalkov[3] and D. J. Mowbray[1 a)]

1. Department of Physics and Astronomy, University of Sheffield, Sheffield S3 7RH, United Kingdom
2. School of Physics and Astronomy, Photon Science Institute, University of Manchester, Manchester, United Kingdom
3. INPAC-Institute for Nanoscale Physics and Chemistry, Pulsed Fields Group, K.U. Leuven, Celestijnenlaan 200D, B-3001 Leuven, Belgium
4. Department of Electronic and Electrical Engineering, University College London, Torrington Place, London WC1E 7JE, United Kingdom
5. Department of Electronic and Electrical Engineering, University of Sheffield, Sheffield S1 3JD, United Kingdom

Abstract

We report a magneto-optical study of InAs-InGaAs-GaAs self-assembled quantum dots (QDs) subjected to post-growth thermal annealing at different temperatures. At low temperatures annealing strongly affects the bimodal distribution of QDs, at higher temperatures a strong blue shift of the emission occurs. Magneto-photoluminescence reveals that the annealing increases the QD size, with a larger effect occurring along the growth axis, and decreases the carrier effective masses. The main contribution to the blue shift is deduced to be an increase in the average Ga composition of the QDs. The inadvertent annealing which occurs during the growth of the upper AlGaAs cladding layer in laser structures is also studied.

[a)] Electronic mail: D.Mowbray@sheffield.ac.uk

I. Introduction

Semiconductor quantum dots (QDs) exhibit a number of unique properties which makes them attractive for the active region of injection lasers. For example, their discrete density of states is predicted to result in reduced threshold current densities (J_{th}) and increased temperature stability [1,2], and the strong spatial localisation of charge carriers reduces the device sensitivity to processing or radiation induced damage [3]. Following over a decade of optimisation, lasers utilising self-assembled quantum dots [4] now demonstrate many advantages [5,6] in comparison to quantum well lasers, despite less than ideal intrinsic properties which include significant inhomogeneous broadening of the optical transitions, multiple confined energy states and a high density of electronic states external to the dots.

Whilst changes to the growth parameters can be used to modify the intrinsic QD properties, including size/composition (and hence emission energy and energy level separations) and density, controlled variation over a wide range can be difficult to obtain. However, a continuous and controllable variation of the emission energy can be achieved by subjecting the QDs to post-growth thermal annealing at temperatures above the growth temperature. This results in a significant blue shift of the emission, with shifts as large as ~300 meV having been reported [7]. Thermal annealing is also found to reduce the separation between the confined energy levels and to decrease the inhomogeneous broadening of the QD ensemble [8]. The majority of previous annealing studies have been performed on InAs QDs grown within a GaAs matrix. The annealing is believed to result in Ga and In diffusion, thereby increasing the Ga content of the QDs. In addition, the effective size of the QDs is believed to increase [9] and the confinement potential softened [10].

Despite a number of reports of the effects of annealing on the properties of In(Ga)As-GaAs QDs, these as-grown dots generally emit significantly below 1.3µm at room temperature and there have been relatively few studies of the effects of annealing on QDs designed to emit at 1.3µm with the required high density for laser applications [11, 12, 13]. In addition, very few optical studies of the effects of annealing have related the observed changes directly to changes in the structural properties [9]. In this paper we report a detailed study of the effects of thermal annealing on the properties of 1.3µm emitting QDs, which have been shown previously to allow the fabrication of lasers with excellent characteristics [14]. The inadvertent annealing that occurs during the growth of the upper AlGaAs cladding layer in laser structures is investigated and magneto-optical studies, in fields up to 50T, are used to probe the physical structure of the annealed QDs.

II. Experimental details

InAs self-assembled QDs were grown in a thin InGaAs-GaAs quantum well (a so-called dot-in-a-well or DWELL structure) by molecular beam epitaxy (MBE) on Si-doped GaAs (100) substrates. Placing the QDs in an InGaAs-GaAs quantum well allows the growth of high density dots emitting at 1.3 μm with a high optical efficiency at room temperature [15]. Two samples are studied in the present work. The first sample contained 5 DWELLs, each consisting of dots formed from 3 monolayers (MLs) of InAs grown within an 8 nm $In_{0.15}Ga_{0.85}As$ quantum well. The growth temperature for the QDs and InGaAs quantum well was 510 °C. Each of the DWELLs was separated by a 50 nm GaAs spacer layer in which the initial 15 nm was grown at 510 °C, with the temperature increased to 580 °C for the remaining 35 nm. This gives the High Growth Temperature Spacer Layer (HGTSL) growth technique which improves the photoluminescence (PL) efficiency for multi-layer QD structures via a reduction in the density of defective QDs [14]. This growth technique has been shown previously to result in 1.3 μm emitting QD lasers with excellent characteristics [16]. The second sample contained only a single DWELL. The as-grown wafers emitted close to 1.3 μm at room temperature. After growth, parts of the wafers were annealed at 650, 700 and 750 °C by rapid thermal annealing (RTA) for 10 minutes. The samples were 'sandwiched' between two GaAs wafers to prevent As loss during the annealing process. PL at 77 K was excited using a 532 nm solid-state laser, dispersed by a 0.75 m monochromator and detected with a liquid nitrogen cooled Ge detector. Magneto-PL spectra were recorded at 4.2 K in fields up to 50 T in a pulsed magnet system. 532 nm exciting light was transmitted to the sample via a 200 μm-core optical fibre, with a bundle of six similar fibres used to collect the resultant PL [17]. The PL was detected by a cooled InGaAs diode array. Up to 23 spectra were obtained during each 20 ms field pulse. Spectra were recorded for the field applied both normal (Faraday geometry) and parallel (Voigt geometry) to the QD plane.

III. Experimental Results

A. Zero-field photoluminescence

Figure 1 shows PL spectra, recorded for a sample temperature of 77 K, for the as-grown five layer sample and the same sample annealed at three different temperatures. Of particular note is the presence of a bimodal emission for both the as-grown sample and the sample annealed at a temperature of 650 °C. The spectra of both samples exhibit a constant form as the excitation power is reduced to very low levels, indicating that the higher energy emission does

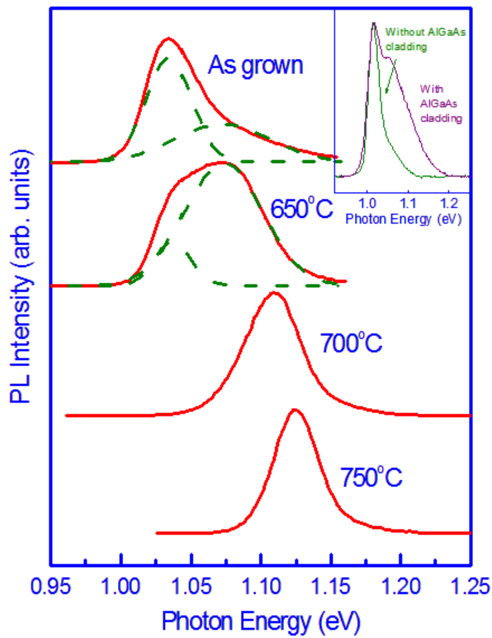

Figure 1. PL spectra recorded for a sample temperature of 77K for the as-gown wafer and three annealing temperatures. The dashed lines are fits to the as-gown and 650 °C sample spectra with two Gaussian functions. The inset shows PL spectra of a test structure consisting of 5 DWELLs but no AlGaAs cladding and a full laser structure with ~1.5µm upper and lower AlGaAs cladding layers.

not result from an excited state transition but instead that the bimodal emission results from the presence of two sub-sets of QDs. Fitting both spectra with two Gaussian functions allows the parameters of these two sub-sets of dots to be determined. This gives central emission energies (line widths) of 1.034(32) and 1.070(72) eV (meV) for the as-grown wafer and 1.036(25) and 1.073(55) eV (meV) for the 650 °C annealed sample respectively. The integrated intensity ratio of the high to low energy emission changes from 0.8 to 5.5 with annealing. Hence annealing at 650 °C has little effect on the emission energies of the two subsets of QDs but reduces their inhomogeneous broadening and significantly alters their relative contribution to the total emission, with the higher energy subset becoming dominant following annealing. A similar effect is observed in as-grown, full laser structures which, in addition to the present structures, contain thick (~1.5 µm) AlGaAs cladding layers grown at 680 °C over a period of ~ 1 hour. The inset to Fig. 1 compares low temperature emission spectra of a multiple DWELL structure, similar to the present structure, and a full laser structure. The addition of the AlGaAs cladding layer is seen to produce a similar change to post-growth annealing at 650 °C, with a relative enhancement of the emission from the higher energy sub-set of QDs.

With increasing temperature the intensity of the emission from the higher energy subset of QDs decreases as carriers are thermally excited to the wetting layer / InGaAs QW and are subsequently recaptured by the lower energy subset of dots. By room temperature the emission is essentially mono-modal, with the lower energy sub-set of QDs giving emission at 1.3 µm. Hence, the higher energy sub-set of dots does not act as a parasitic recombination channel at high temperatures but, assuming a constant total number of QDs, their presence in the structure acts to reduce the number of dots emitting at 1.3 µm, and hence the maximum gain available in a laser device. If the emission at 77 K represents the full distribution of QD sizes then it is

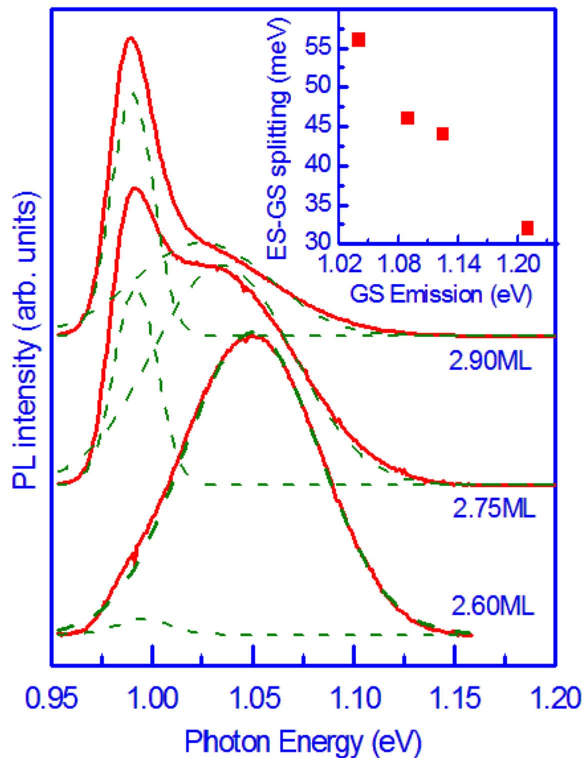

Figure 2. 4.2K PL spectra of three single DWELL structures with different amounts of InAs deposited to form the QDs. Fits to each spectra with two Gaussian functions are shown by dashed lines. The inset plots the excited state – ground state energy separation as a function of absolute ground state emission energy for a single DWELL structure both as-grown and annealed at different temperatures.

possible to estimate the fraction of QDs emitting in a small band around 1.3 µm. This decreases by a factor of ~1.8 between the as-grown and 650 °C annealed samples. These results indicate that the growth conditions of the upper AlGaAs cladding layer are critical for optimum device performance, with a high temperature needed for high quality AlGaAs, but too high a temperature resulting in a decrease in the number of dots able to contribute to 1.3 µm lasing at room temperature.

The change in the QD emission properties when annealed at relatively low temperatures (650 °C) appears to be related to the loss of small amounts of InAs from the dots. Fig. 2 shows low temperature PL spectra of three single layer DWELL structures (grown without AlGaAs cladding layers) for different amounts of InAs (2.60, 2.75 and 2.90 ML) deposited to form the QDs [15]. All three samples exhibit a bimodal emission, with the emission intensity shifting from the high to low energy sub-set of QDs as the amount of deposited InAs is increased. It is seen that reducing the amount of InAs deposited results in a significant increase in the relative strength of the emission from the higher energy subset of dots, similar to the behaviour observed when annealing at 650 °C.

Annealing at 650 °C produces relatively little change in the emission energies of the QDs (2 and 3 meV for the low and high energy subsets respectively). However, with increasing annealing temperature a significant blue shift occurs, with a maximum blue shift of 90 meV obtained for a temperature of 750 °C. By increasing the excitation power, emission from the first excited state is observed, allowing the ground state – excited state separation to be determined. This separation is plotted against the ground state emission energy for different annealing temperatures in the inset to Fig. 2 for the single layer sample. For this sample it is

easier to observe, and hence to more accurately determine, the excited state emission. However the ground state emission of this sample shifts more rapidly with annealing temperature than occurs for the five layer sample, for reasons that are not totally clear. For example, the shift between the as-grown wafer and the 750 °C annealed sample is 180 meV for the single layer structure compared to 90 meV for the five layer sample. The data plotted in the inset to Fig. 2 indicates that the excited state shifts less rapidly with annealing than does the ground state. For the present data the ratio of these shifts (excited state : ground state) is determined to be 0.86.

B. Magneto-PL

The application of a magnetic field to a semiconductor nanostructure provides a known perturbation of the electronic structure, allowing information on the size of the exciton, and hence size of the nanostructure, and carrier effective masses to be determined. For low magnetic fields the field provides a perturbation weaker than the exciton binding energy and the emission energy increases quadratically with field. This diamagnetic behaviour is given by $\Delta E_{e,h} = e^2 \langle \rho_{e,h}^2 \rangle B^2 / 8m_{e,h}$ where $\sqrt{\langle \rho_i^2 \rangle}$ and m_i are the electron (hole) effective wave function radius and mass in the plane perpendicular to the field direction and $\Delta E_{e,h}$ is the field induced shift of the electron or hole states. In this regime the exciton size is determined by the physical size of the QD. For high fields the magnetic perturbation exceeds the exciton binding energy and a linear Landau shift $\hbar eB / 2m_{e,h}$ of the emission energy occurs, with a small correction for the exciton binding energy, $-\hbar^2 / 2\mu \langle \rho^2 \rangle$, where μ is the reduced mass of the exciton. By fitting the experimentally determined shift of the emission using a function of the form:

$$E = E_0 + \frac{e^2 \langle \rho^2 \rangle B^2}{8\mu} \quad \text{for} \quad B < \frac{2\hbar}{e\langle \rho^2 \rangle}$$

$$E = E_0 - \frac{\hbar^2}{2\mu \langle \rho^2 \rangle} + \frac{\hbar eB}{2\mu} \quad \text{for} \quad B > \frac{2\hbar}{e\langle \rho^2 \rangle}$$

where E_0 is the emission energy for zero field and both parts of the equation and their derivatives are constrained to be continuous at the boundary field $B = \frac{2\hbar}{e\langle \rho^2 \rangle}$, it is possible to determine values for μ and $\sqrt{\langle \rho^2 \rangle}$, the exciton effective mass and effective radius [17,18]. The

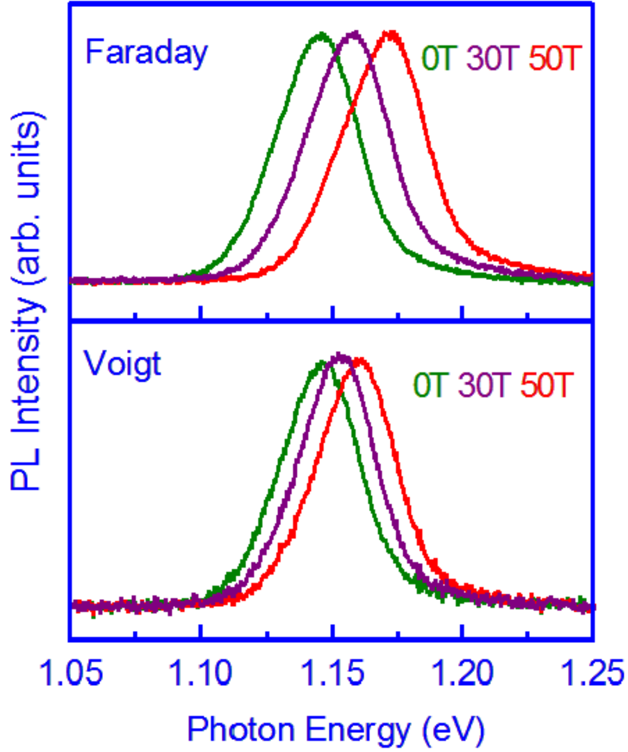

Figure 3. PL spectra recorded for 0, 30 and 50T for the 750 °C annealed sample in both the Faraday and Voigt geometries.

transition between the diamagnetic and linear behaviour occurs when the magnetic length $l_0 = \sqrt{\hbar / eB}$ becomes comparable to the QD size. To determine both the exciton radius and reduced mass both the quadratic and linear regimes must be observed, requiring the use of high magnetic fields for nanostructures with a small spatial size. In the present analysis it is assumed that $\rho_e=\rho_h$; this is believed to be a reasonable assumption when both carrier types are localised in the QD [18]. The value extracted for $\sqrt{\langle \rho_i^2 \rangle}$ will be the smallest dimension in the plane normal to the applied field. In general, for self-assembled QDs the dot height is significantly less than the base length and hence it is the latter dimension which is determined in the Faraday geometry (field applied along the growth axis) but the former in the Voigt geometry (field applied normal to the growth axis). However in the present dots it will be seen that the two dimensions extracted from the magneto-PL are in some cases comparable.

Figure 3 shows representative spectra of the emission from the 750°C annealed sample as a function of magnetic field and for both the Faraday and Voigt geometries. As expected a blue shift of the emission is observed with increasing field, with a larger shift observed for the Faraday geometry. Figure 4 plots the magnetic field induced shift of the emission at 4.2 K for the as-grown, 700 and 750°C annealed samples for both the Faraday and Voigt geometries. Data for the 650 °C shows similar trends but is omitted from the figure to aid clarity. For all samples a larger shift is observed for the Faraday geometry, consistent with a larger value for the combination $\langle \rho^2 \rangle / \mu$ in this geometry. With increasing annealing temperature a larger field induced shift of the emission is observed for both geometries. Referring to the above equations this behaviour indicates that annealing either increases the physical size of the quantum dots or

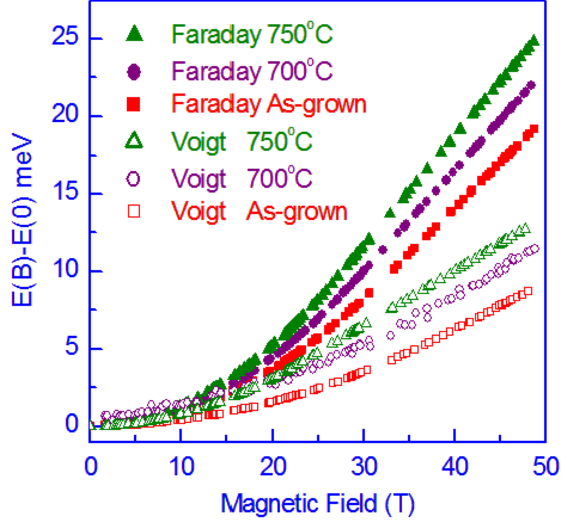

Figure 4. Energy shift as a function of magnetic field for the as-grown and 700 and 750 °C annealed 5 DWELL structure. For clarity data for the 650 °C sample is omitted from the figure. Closed (open) symbols refer to the Faraday (Voigt) geometry. The sample temperature for the measurements is 4.2K.

reduces the carrier effective mass, or a combination of both effects. Table I summarises the parameters extracted from the experimental data by fitting with the above equations.

IV. Discussion of results

Previous magneto-optical studies of single layers or uncoupled multiple layers of InAs QDs grown within a GaAs matrix have been able to determine parameters for the Faraday geometry. However, for the Voigt geometry the relatively small height of the dots generally prevents the high field limit $B > \frac{2\hbar}{e\langle\rho^2\rangle}$ being attained over a sufficiently large field range, hence preventing a determination of the reduced mass and the extent of the exciton along the growth axis [17,19,20]. In the present studies the high field limit is reached for both geometries at relatively low fields, allowing a comparison of inplane and growth direction parameters.

	Faraday		Voigt	
Sample	μ / m_0	a_B / nm	μ / m_0	a_B / nm
As grown	0.099±0.002	6.41±0.06	0.190±0.015	5.8±0.2
650°C	0.095±0.002	6.73±0.05	0.186±0.008	6.31±0.1
700°C	0.089±0.002	6.73±0.05	0.185±0.007	6.6±0.1
750°C	0.082±0.002	7.00±0.06	0.165±0.008	7.6±0.1

Table I. Parameters extracted from fits to the magneto-PL data for the as-grown and annealed samples.

For the as-grown and all annealed samples the inplane (Faraday geometry) reduced exciton mass is approximately half that of the growth direction (Voigt geometry) mass. The ground hole state in the QD is calculated to have a predominantly heavy-hole like character [21] and for the majority of III-V semiconductors the heavy-hole mass is significantly greater than the electron mass; this results in a reduced exciton mass close to that of the electron. However, in quantum wells the mass of the highest hole state reverses for motion normal to the

growth axis and for small wave vectors, with the mass being much smaller than the growth direction heavy hole mass [22,23]. For bulk InAs calculations give a mass reduced by a factor ~10, for GaAs the reduction is by a factor ~3.5 [24]. A similar behaviour in QDs, which because of their smaller height than base length behave in many cases like quantum wells, would explain the different Voigt and Faraday determined reduced masses. The Faraday geometry reduced mass would represent the combination of the electron mass and a small hole mass, with the Voigt mass being close to that of the electron. The present masses determined for the Faraday geometry are reasonably consistent, although slightly lower, than values (0.11~0.13m_0) previously reported for InAs QDs and determined using the same magneto-PL technique [17,19]. However, if the Voigt geometry mass does reflect that of the electron it appears rather large, for example Pryor [24] calculates a spatially averaged electron mass in InAs QDs of ~0.042m_0 although it is unclear if this includes enhancements due to non-parabolicity. The inclusion of any Ga within the QDs (even intentional InAs QDs have been shown to contain significant amounts of Ga [25]) may also enhance the electron mass. Awirothananon et al [26] have reported a reduced mass of ~0.066m_0 for as grown InAs-GaAs QDs from the measured Zeeman splitting of the first excited state.

The magneto-PL results give a direct determination of the physical size of the exciton. Although the exciton size has been shown previously to be proportional to the physical size of the QDs [27] the coefficient of proportionality will depend on the precise nature of the confined wavefunctions. Hence, in the following we make no attempt to deduce absolute QD sizes but instead use the magneto-PL data to probe fractional changes in the QD size due to annealing. Only relatively low resolution structural images of as-grown DWELL structures are available, hence a precise determination of the size of the as-grown QDs is not possible. However from available transmission electron microscope (TEM) images approximate values for the base length and height of 17 and 6nm respective can be extracted [14].

Thermal annealing of InAs QDs will result in a number of changes to their physical and electronic structure. The potential profile will change as Ga diffuses into the dots, resulting in larger effective dots with a smoother potential variation at the interfaces. In addition, an increased Ga composition will decrease the strain state of the dots and increase the effective band gap. Furthermore both the direct change in composition and change in strain will alter a number of parameters, including the carrier effective masses. For both geometries (Faraday and Voigt) annealing is seen to increase the size of the exciton and this is assumed to reflect an increase in the physical size of the quantum dots. However this effect is much larger for the height of the QD (Voigt data) where an increase of 31% is observed between the as-grown and

750 °C annealed sample, compared to only a 9% increase for the inplane dimensions (Faraday data).

Between the as-grown sample and the sample annealed at 750 °C the magneto-PL data indicates increases in both spatial dimensions of 9% (inplane) and 31% (growth direction) and decreases in the effective masses of 17% (inplane) and 13% (growth axis). The former increases will act to decrease the emission energy whilst the latter decreases will act to increase it. To estimate the effects of small variations in the QD size we use the calculations of Pryor [28] for truncated pyramidal QDs, which provide a reasonable approximation to the shape of the present dots. In these calculations the energies of the confined QD states are found to be relatively insensitive to the dot height, a behaviour attributed to the counteracting effects of strain and confinement. Hence it is the change in the inplane dimension that makes the major contribution to the confined energy levels, an increase of 9% from an initial value of 17nm is calculated to decrease the confinement energies contributing to the lowest energy transition by 10%, corresponding to an absolute shift of 28 meV [28]. If it is assumed that the confinement energies scale inversely with the reduced mass then the effect of the average decrease of the reduced masses (~15%) will almost fully compensate the size induced shift.

The calculations of [28] also show the first excited state transition to be more sensitive to changes in the inplane dot size than the ground state transition. The data plotted in the inset to Fig. 2 is for the single layer sample for which no magneto-PL data is available. However, as the PL for this sample shifts twice as much with annealing as it does for the multiple layer sample, it is assumed the changes in the QD dimensions are twice as great. Using the calculations of [28] the ground state and first excited state transition separation is predicted to decrease by 17 meV between the as-grown and most annealed sample, in reasonable agreement with the measured decrease of 24 meV.

The above considerations indicate that changes to the physical size and reduced exciton mass resulting from annealing effectively cancel, this leaves changes to the composition as the main factor contributing to the strong annealing-induced blue shift of the emission. Only a very approximate estimate of this effect can be made as the composition is expected to be very non-uniform. Pryor and Pistol [29] calculate the band edge energies of QDs grown on a range of different substrates. For InGaAs QDs grown on a GaAs substrate the effective band gap changes by ≈680 meV as the dot composition changes from pure InAs to pure GaAs. Hence based on these calculations the 90meV shift observed when annealing the multi-layer sample at 750 °C corresponds to an absolute increase in the Ga composition of ≈ 0.13.

Given this increase in the average Ga composition of the QDs, the measured decrease in the reduced masses is difficult to understand. For unstrained, bulk $In_{1-x}Ga_xAs$ the electron mass increases from 0.023 to 0.067m_0 (190% increase) as the composition x varies from 0 to 1. Calculations for strained InGaAs QDs grown on GaAs predict a weaker (20%) increase [24] but the sign of this change (increasing as the Ga content is increased) is still opposite to that determined experimentally (~ -15%, see table I). The reason for this behaviour is unclear but we note that a weak decrease in the electron effective mass was also observed by Awirothananon et al [26] when annealing InAs QDs.

V. Conclusions

Optical and magneto-optical spectroscopy has been used to probe the electronic and structural properties of thermally annealed InAs QDs grown within an InGaAs-GaAs quantum well. Annealing is found to increase the effective size of the dots, with a significantly larger increase occurring along the growth direction in comparison to the inplane direction. The exciton reduced mass decreases with annealing, the opposite effect to that expected from the deduced increase in average Ga content of the QDs. The increased QD size and decreased mass affect the transition energies in opposite directions, and in the present studies these two contributions approximately cancel. Hence the main contribution to the blue shift of the emission is an increased Ga composition of the QDs. For low annealing temperatures there is little change in the emission energy of the QDs but a strong redistribution between the emission from two subsets of different size QDs. Low annealing temperatures makes the QD ensemble more bimodal. A similar effect is seen in full laser structures where annealing of the QDs occurs during the growth of the upper AlGaAs cladding layer.

VI. Acknowledgements

This work is supported by the U.K. Engineering and Physical Sciences Research Council (EPSRC), grant GR/S49308/01, and the European Commission Network of Excellence SANDiE, contract NMP4-CT-2004-500101. The work at the KU Leuven is supported by the IAP, GOA and FWO programmes.

References

[1] Y Arakawa and H Sakaki Appl. Phys. Lett. **40**, 939, (1982).

[2] M Asada, Y Miyamoto and Y Suematsu, IEEE J. Quant. Electron. QE-**22**, 1915, (1986).

[3] P G Piva, R D Goldberg, I V Mitchell, D Labrie, R Leon, S Charbonneau, Z R Wasilewski and S Fafard, Appl. Phys. Lett. **77,** 624 (2000)

[4] D Bimberg, M Grundmann and N N Ledentsov in Quantum Dot Heterostructures John Wiley and Sons (1999)

[5] S Freisem, G Ozgur, K Shavritranuruk, H Chen and D G Deppe, Electron. Lett. **44,** 679 (2008).

[6] T J Badcock, R J Royce, D J Mowbray, M S Skolnick, H Y Liu, M Hopkinson, K M Groom and Q Jiang, Appl. Phys. Lett. **11,** 111102 (2007).

[7] S Malik, C Roberts, R Murray and M Pate. Appl. Phys. Lett. **71,** 1987 (1997)

[8] S Fafard and C N Allen, Appl. Phys. Lett. **75,** 2374 (1999)

[9] A O Kosogov, P Werner, U Goesele, N N Ledentsov, D Bimberg, V M Ustinov, A Yu Egorov, A E Zhukov, P S Kop'ev, N A Bert and Zh I Alferov, Appl. Phys. Lett. **69,** 3072 (1996).

[10] R Santoprete, P Kratzer, M Scheffler, R B Capaz and B Koiller, J. Appl. Phys. **102,** 023711 (2007).

[11] T Yang, J Tatebayashi, K Aoki, M Nishioka and Y Arakawa, Appl. Phys. Lett. **90,** 111912 (2007)

[12] J Tatebayashi, Y Arakawa, N Hatori, H Ebe, M Sugawara, H Sudo and A Kuramata, Appl. Phys. Lett. **85,** 1024 (2004).

[13] S Malik, E C Le Ru, D Childs and R. Murray, Phys. Rev. B. **65,** 155313 (2001)

[14] H Y Liu, I R Sellers, T J Badcock, D J Mowbray, M S Skolnick, K M Groom, M Gutiérrez, M Hopkinson, J S Ng, J P R David and R Beanland. Appl. Phys. Lett. **85,** 704 (2004).

[15] H Y Liu , M Hopkinson , C N Harrison , M J Steer, R Frith, I R Sellers, D J Mowbray and M S Skolnick, J. Appl. Phys. **93,** 2931 (2003).

[16] I R Sellers, H Y Liu, K M Groom, D T Childs, D Robbins, T J Badcock, M Hopkinson, D J Mowbray and M S Skolnick, Electron. Letts. **40,** 1412 (2004).

[17] S Godefroo, J Maes, M Hayne, V V Moshchalkov, M Henini, F Pulizzi, A Patanè and L Eaves, J. Appl. Phys. **96,** 2535 (2004).

[18] M Hayne, R Provoost, M K Zundel, Y M Manz, K Eberl and V V Moschalkov, Phys. Rev. B. **62,** 10324 (2000).

[19] J Maes M Hayne, M Henini, F Pulizzi, A Patanè, L Eaves and V V Moshchalkov, Physica B **346,** 428 (2004).

[20] An exception to this is T Nuytten, M Hayne, M Henini and V V Moshchalkov, Phys. Rev. B. 77, 115348 (2008), where the high field limit was achieved in the Voigt geometry for InAs/GaAs self-assembled QDs, although at insufficiently low fields to allow a full analysis of the corresponding data.

[21] G A Narvaez, G Bester and Alex Zunger, J. Appl. Phys. **98**, 043708 (2005)

[22] C Weisbuch, Semiconductors and Semimetals **24,** 1 Academic Press (1987)

[23] A S Plaut, J Singleton, R J Nicholas, R T Harley, S R Andrews and C T B Foxon, Phys. Rev. B. **38,** 1323 (1988).

[24] C Pryor Phys. Rev. B. **57,** 7190 (1998)

[25] P W Fry, I E Itskevich, D J Mowbray, M S Skolnick, J J Finley, J A Barker, E P O'Reilly, L R Wilson, I A Larkin, P A Maksym, M Hopkinson, M Al-Khafaji, J P R David, A G Cullis, G Hill and J C Clark, Phys. Rev. B. **84,** 733 (2000)

[26] S Awirothananon, W D Sheng, A Babinski, S Studenikin, S Raymond, A Sachrajda, M Potemski, S Fafard, G Ortner and M Bayer, Jap. J. Appl. Phys. **43,** 2088 (2004).

[27] M Sugisaki, H-W Ren, S V Nair, K Nishi and Y. Masumoto, Phys. Rev. B **66,** 235309 (2002).

[28] C E Pryor, Phys. Rev. B. **60,** 2869 (1999).

[29] C E Pryor and M-E Pistol, Phys. Rev. B. **72,** 205311 (2005).